semiconductor dielectric integrated circuits," *IEEE Trans Microwave Theory Tech.*, vol. MTT-22, pp 411–417, Apr. 1974.
[6] R. M Knox and P. P. Toulois, "A V-band receiver using image line integrated circuits," *Proc Nat. Electronics Conf.*, vol 27, pp. 489–492, Oct. 1974
[7] H. Jacobs, G Novick, C. M. LoCascio, and M. M. Chrepta, "Measurement of guided wavelength in rectangular dielectric waveguides," *IEEE Trans Microwave Theory Tech.*, vol MTT-24, pp 815–820, Nov. 1976.
[8] R. E Collin and F. J. Zucker, *Antenna Theory*, vol 2 New York: McGraw-Hill, 1969, ch 19, 20
[9] R E. Collin, *Field Theory of Guided Waves*, ch 9 New York: McGraw-Hill, 1960

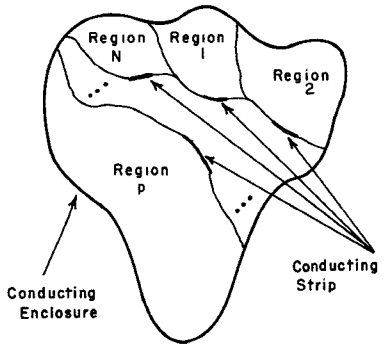

Fig 1. Generic cross section of mixed conductors and dielectrics in conducting enclosure

Dispersion Characteristics for Arbitrarily Configured Transmission Media

ACHINTYA K. GANGULY AND
BARRY E. SPIELMAN, MEMBER, IEEE

***Abstract*—A method for calculating the propagation characteristics of electromagnetic waves along arbitrarily configurated transmission media composed of conductors and/or inhomogeneous dielectrics is presented. The method is based on the equivalence principle. The dispersion characteristics of the fundamental as well as higher order modes can be obtained by this method. To demonstrate the validity of this method, results of the propagation constant of a shielded microstrip line calculated by this method are compared with other numerical results available in the literature. New results for the dispersion characteristics of a channelized suspended microstrip are presented.**

I. Introduction

The success of microstrip in microwave integrated-circuit applications has caused considerable interest in the calculation of dispersion characteristics of these lines. A number of different techniques [1]–[4] have been employed to obtain dispersive effects of open and shielded microstrip-like transmission lines with rectangular cross sections. Since microstrip becomes lossy and difficult to fabricate at higher microwave frequencies, attention has focused on configuring new transmission media. In this short paper we present a technique for calculating the dispersion characteristics of electromagnetic wave propagation along guiding structures consisting of a finite number of uniform dielectric regions of arbitrary cross sections within a conducting enclosure. Conducting strips may also be present at the interface between two dielectric regions. It is assumed that the thickness of the conductors is negligible.

In Section II the problem is formulated on the basis of the equivalence principle. A set of linear integro-differential operator equations for the equivalent current sources are obtained by applying the appropriate boundary conditions at each interface. In Section III the method for converting the operator equations into a matrix formulation by the method of moments [6, pp. 9–11, 14, 15] is sketched. The numerical methods used to determine the propagation characteristics and results for specific examples are described in Section IV.

Manuscript received May 20, 1977; revised July 13, 1977
The authors are with the Naval Research Laboratory, Washington, DC 20375.

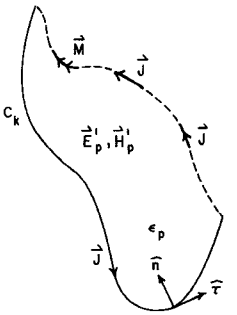

Fig 2 Conceptual treatment of currents and fields for the pth region $\hat{\tau}$, $\hat{n}$, and $\hat{z}$ are unit vectors along three orthogonal coordinates axes used in the text $\hat{z}$ is normal to the plane of the paper pointing up.

II. Integro-Differential Equations

Fig. 1 shows the generic cross section of the guiding structure under consideration. N is the number of discrete, homogeneous, isotropic, dielectric regions inside the conducting enclosure. The heavy lines on the interface between two dielectric regions denote conducting strips. The electric ($\boldsymbol{E}$) and magnetic ($\boldsymbol{H}$) fields in each region will be obtained by applying the principle of equivalence [5]. In accordance with this principle, the dielectric medium of the pth region (characterized by permittivity ε_p) is fictitiously extended to fill all space and combinations of electric ($\boldsymbol{J}^p$) and magnetic ($\boldsymbol{M}^p$) surface current sources are conceptually placed on the boundary S_p of the pth region. $\boldsymbol{J}^p$ and $\boldsymbol{M}^p$ are to be determined in such a way that $\boldsymbol{E}$ and $\boldsymbol{H}$ are zero everywhere outside S_p and are identical to the fields $\boldsymbol{E}^p$ and $\boldsymbol{H}^p$ at each point in the interior of the pth region for the original problem shown in Fig. 1. This procedure is repeated for each of the regions inside the conducting enclosure. The current sources for the various regions are not all independent because of the boundary conditions to be satisfied at all the interfaces. Fig. 2 symbolically shows the contour of the pth region and the surface current distributions on it. $\boldsymbol{M}^p$ is taken to be zero on the conducting segments of the boundary. Also shown in Fig. 2 is a left-handed coordinate system with unit vectors $\hat{\tau}_p$, $\hat{n}_p$, and $\hat{z}$. $\hat{\tau}_p$ is tangential to the contour c_p (counterclockwise), $\hat{n}_p$ inward drawn normal to the region p, and $\hat{z}$ perpendicular to the plane of Fig. 2. For two adjacent regions p and p', we have $\hat{\tau}_p = -\hat{\tau}_{p'}$ and $\hat{n}_p = -\hat{n}_{p'}$ on the portion of boundary common to both the contours c_p and $c_{p'}$. $\hat{z}$ is the same for all regions. Since $\boldsymbol{J}^p$ and $\boldsymbol{M}^p$ are surface currents, we have the relations

$$\hat{n}_p \cdot \boldsymbol{M}^p = 0$$
$$\hat{n}_p \cdot \boldsymbol{J}^p = 0. \tag{1}$$

From the equivalence principle

$$J^p(\rho,z) = \hat{n} \times H^{p-}(\rho,z)$$
$$M^p(\rho,z) = -\hat{n} \times E^{p-}(\rho,z) \quad (2)$$

where E^{p-} and H^{p-} denote, respectively, the electric and magnetic fields at a point just inside the contour c_p. ρ is a position vector in the transverse plane. In (2), ρ is on c_p.

From Maxwell's equations, the electric (E^p) and magnetic (H^p) fields at any point in the cross section of Fig. 2 may be written as

$$-\varepsilon_p E^p = \nabla \times F^p + j\varepsilon_p \omega A^p + \varepsilon_p \nabla \phi_e^p \quad (3)$$

$$-\mu_0 H^p = -\nabla \times A^p + j\mu_0 \omega F^p + \mu_0 \nabla \phi_m^p \quad (4)$$

where $p = 1, 2, \cdots, N$. A^p and ϕ_e^p are the vector and scalar potentials, respectively, due to the electric current sources (J^p) residing on the contour c_p. Similarly, F^p and ϕ_m^p are the vector and scalar potentials, respectively, due to the magnetic current sources (M^p) residing along c_p. μ_0 is the free-space permeability. In (3) and (4) a time dependence of $e^{i\omega t}$ has been assumed for the sources.

The potentials A, F, ϕ_e, and ϕ_m are given by

$$A^p(\rho,z,t) = \mu_0 e^{+i\omega t} \int_{c_p} J^p(\rho',z) G(k_\rho^p R)\, d\tau' \quad (5)$$

$$F(\rho,z,t) = \varepsilon_p e^{+i\omega t} \int_{c_p} M^p(\rho',z) G(k_\rho^p R)\, d\tau' \quad (6)$$

$$\phi_e^p(\rho,z,t) = -(1/j\omega\varepsilon_p) e^{i\omega t} \cdot \int_{c_p} \nabla' \cdot J^p(\rho',z,t) G(k_\rho^p R)\, d\tau' \quad (7)$$

$$\phi_m^p(\rho,z,t) = -(1/j\omega\mu_0) e^{i\omega t} \cdot \int_{c_p} \nabla' \cdot M^p(\rho',z,t) G(k_\rho^p R)\, d\tau' \quad (8)$$

where $R = |\rho - \rho'|$ is the distance between a field point (ρ) and a source point (ρ'), $k_\rho^p = |\mu_0 \varepsilon_p \omega^2 + k_z^2|^{1/2}$, and $G(k_\rho^p R)$ is the two-dimensional Green's function. If $(\mu_0 \varepsilon_p \omega^2 + k_z^2)$ is positive, $G(x)$ can be expressed in terms of $H_0^{(2)}(x)$, the zero-order Hankel function of the second kind, as

$$G(x) = (1/4j) H_0^{(2)}(x) \quad (9)$$

while for $(\mu\varepsilon_p \omega^2 + k_z^2)$ negative

$$G(x) = (1/2\pi) K_0(x) \quad (10)$$

where $K_0(x)$ is the zero-order modified Bessel function.

The gradient operators ∇ and ∇' operate on the field points and the source points, respectively. The operator ∇' may be written as

$$\nabla' = \nabla_t' + \hat{z} \frac{\partial}{\partial z} \quad (11)$$

where ∇_t' is the tangential part of the vector. The electric (E^p) and magnetic (H^p) fields in the pth region can be calculated by substituting (5)–(10) in (3) and (4). We assume that the sources vary as $e^{-k_z z}$ along the z-axis. For lossless propagation $k_z = i\beta$. By using the one-dimensional divergence theorem terms like $(\nabla_t' \cdot J^p)G$ in (7) and (8) may be expressed in the form $J^p \cdot \nabla_t' G$. Furthermore, we have

$$\nabla_t' G(k_\rho^p R) = -\nabla_t G(k_\rho^p R) = -\hat{R} k_\rho^p \frac{\partial G(x)}{\partial x} \quad (12)$$

where $x = k_\rho^p R$ and $\hat{R} = (\rho - \rho')/R$ is the unit vector from the source point (ρ') to the field point (ρ). Using these relations and after some vector manipulations the tangential components of E^p and H^p at a point P_- just inside the contour c_p may be expressed in the following form:

$$E_z^{p-} = j\mu_0\omega \left[-\int d\tau' J_{z'}^p G(x) \left\{ 1 + \frac{k_z^2}{\bar{\varepsilon}_p k_0^2} \right\} + \frac{k_z k_\rho^p}{\bar{\varepsilon}_p k_0^2} \int d\tau' J_{\tau'}^p \hat{\tau}' \cdot \hat{R} G'(x) + \frac{k_\rho^p}{k_0} \int d\tau' \hat{n}' \cdot \hat{R} G'(x) \tilde{M}_{\tau'}^p \right] \quad (13)$$

$$E_\tau^{p-} = j\mu_0\omega \left[\int d\tau' \frac{k_z k_\rho^p}{\bar{\varepsilon}_p k_0^2} \hat{\tau} \cdot \hat{R} G'(x) J_{z'}^p - \int d\tau' J_{\tau'}^p \left\{ (\hat{\tau}' \cdot \hat{\tau}) \left(G(x) + \frac{k_\rho^p}{\bar{\varepsilon}_p k_0^2 R} G'(x) \right) + \frac{(k_\rho^p)^2}{\bar{\varepsilon}_p k_0^2} (\hat{\tau}' \cdot \hat{R})(\hat{\tau} \cdot \hat{R}) \cdot \left(G''(x) - \frac{1}{k_\rho^p R} G'(x) \right) \right\} - \frac{k_\rho^p}{k_0} \int d\tau' G'(x)(n \cdot R) \tilde{M}_{z'}^p + \frac{k_z}{k_0} \int d\tau' (\hat{n}' \cdot \tau) G(x) \tilde{M}_{\tau'}^p \right] \quad (14)$$

$$H_z^{p-} = (\mu_0 \varepsilon_0)^{1/2} \omega \left[-\frac{k_\rho^p}{k_0} \int d\tau' J_{\tau'}^p \hat{n}' \cdot \hat{R} G'(x) + \bar{\varepsilon}_p \left(1 + \frac{k_z^2}{\bar{\varepsilon}_p k_0^2} \right) \int d\tau' \tilde{M}_{z'}^p G(x) - \frac{k_z k_\rho^p}{k_0^2} \int d\tau' \tilde{M}_{\tau'}^p \hat{\tau}' \cdot \hat{R} G'(x) \right] \quad (15)$$

$$H_\tau^{p-} = (\mu_0 \varepsilon_0)^{1/2} \omega \left[\frac{k_\rho^p}{k_0} \int d\tau' J_{z'}^p (\hat{n} \cdot R) G'(x) - \frac{k_z}{k_0} \int d\tau' J_{\tau'}^p \hat{n}' \cdot \hat{\tau} G(x) - \frac{k_z k_\rho^p}{k_0^2} \int d\tau' \tilde{M}_{z'}^p \hat{\tau} \cdot \hat{R} G'(x) + \bar{\varepsilon}_p \int d\tau' \tilde{M}_{\tau'}^p \left\{ (\hat{\tau} \cdot \hat{\tau}') \left[G(x) + \frac{k_\rho^p}{\bar{\varepsilon}_p k_0^2 R} G'(x) \right] + \frac{(k_\rho^p)^2}{\bar{\varepsilon}_p k_0^2} (\hat{\tau}' \cdot \hat{R})(\hat{\tau} \cdot \hat{R}) \left[G''(x) - \frac{1}{k_\rho^p R} G'(x) \right] \right\} \right]. \quad (16)$$

Here we have replaced the variable M by $\tilde{M}$, where

$$\tilde{M}^p = -j(\varepsilon_0/\mu_0)^{1/2} M^p \quad (17)$$

so that $\tilde{M}^p$ is of the same dimension as J^p. $\bar{\varepsilon}_p = \varepsilon_p/\varepsilon_0$ is the relative dielectric constant of the pth region. $k_0 = \omega\sqrt{\mu_0 \varepsilon_0}$ is the free-space wave vector. $(\hat{n},\hat{\tau},\hat{z})$ and $(\hat{n}',\hat{\tau}',\hat{z}')$ denote unit vectors at the field point (P) and the source points (P'), respectively. Also $G'(x) = \partial G(x)/\partial x$ and $G''(x) = \partial^2 G/\partial x^2$ with $x = k_\rho^p R$.

If the dielectric medium of the pth region is fictitiously extended to all space, then the tangential components of the fields at a point P_+ just outside the contour c_p are given by (see (2))

$$E_z^{p+} = E_z^{p-} + j(\mu_0/\varepsilon_0)^{1/2} \tilde{M}_\tau^p$$
$$E_\tau^{p+} = E_\tau^{p-} - j(\mu_0/\varepsilon_0)^{1/2} \tilde{M}_z^p \quad (18)$$
$$H_z^{p+} = H_z^{p-} - j(\varepsilon_0/\mu_0)^{1/2} J_\tau^p$$
$$H_\tau^{p+} = H_\tau^{p-} + j(\varepsilon_0/\mu_0)^{1/2} J_z^p. \quad (19)$$

Equations (13)–(19) for the tangential components of E^p and H^p hold for each of the dielectric regions $p = 1, 2, \cdots, N$.

The following boundary conditions are now imposed for each of the N dielectric regions in the problem at hand. On the conducting surfaces

$$E_z^{p-} = 0$$
$$E_\tau^{p-} = 0 \tag{20}$$

and on the dielectric–dielectric interfaces

$$E_z^{p+} = 0$$
$$E_\tau^{p+} = 0 \tag{21}$$
$$E_z^{p-} - E_{z'}^{p'-} = 0$$
$$E_\tau^{p-} + E_{\tau'}^{p'-} = 0$$
$$H_z^{p-} - H_{z'}^{p'-} = 0$$
$$H_\tau^{p-} + H_{\tau'}^{p'-} = 0 \tag{22}$$

where E and H are given by (13)–(19). The region p' is adjacent to the pth region in the structure shown in Fig. 1. On the portion of the contour common to regions p and p', $\hat{\tau}' = -\hat{\tau}$, and $\hat{z}' = \hat{z}$. In (20)–(22), $p = 1, 2, \cdots, N$. Also for each p in (22), $p' = 1, 2, \cdots, N_p$ where N_p is the number of regions adjoining the pth region.

On substitution of (13)–(19) in (20)–(22), we obtain the set of integral equations to be satisfied by the current sources J^p, M^p in all regions. J^p and M^p in the different regions are not all independent because of the boundary conditions in (22). From (2) and (22) it is seen that

$$\tilde{M}^p = -\tilde{M}^{p'}$$
$$J^p = -J^{p'}$$

on the dielectric–dielectric interfaces.

III. Matrix Formulation

The propagation characteristics are determined by solving the system of (13)–(22). These equations are reduced to matrix form by the method of moments [6, p. 11]. The moment solution employed here consists of using pulse expansion functions for a basis and point matching for testing. Upon invoking this solution it is found that the matrix equations for all the N different dielectric regions and for all distinct pairs of adjacent regions can be manipulated in such a way that the current sources on the dielectric segments are expressed in terms of $\bar{S}$, the current sources on the conductor segments and then a matrix equation involving $\bar{S}$ only is obtained:

$$H\bar{S} = 0. \tag{23}$$

In (23), $\bar{S}$ is a one-column vector with M components given by

$$M = 2 \sum_{p=1}^{N} n_c^p \tag{24}$$

and H is an $M \times M$ matrix. Here, n_c^p is the number of conductor segments on c_p, obtained by subdividing c_p into straight-line segments (not necessarily of equal length) for the moment solution. The elements of H are functions of only the operating frequency, phase constant, configuration geometry, and material parameters for a given structure. If the cross section of the guiding structure is symmetrical about an axis in the transverse plane, then the problem can be reduced to modes having either even or odd symmetry with respect to this axis. Because of the resulting smaller dimension of the matrix H for each of these modes, the computation time is reduced.

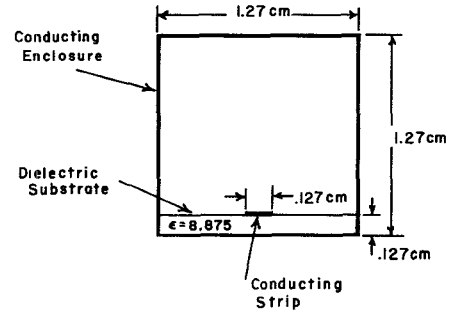

Fig. 3. Cross section for microstrip in a conducting box.

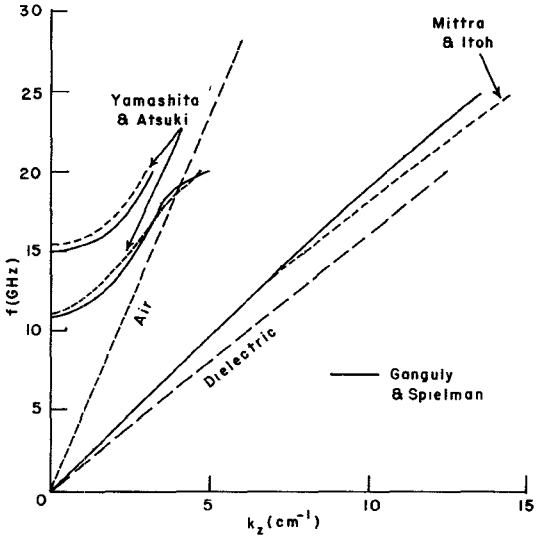

Fig. 4 Dispersion characteristics for microstrip in a conducting box

IV. Numerical Results

Since the components of the vector $\bar{S}$ in (23) are all independent, a solution exists if and only if

$$\det |H(f,k_z)| = 0 \tag{25}$$

where $f = \omega/2\pi$ is the operating frequency and k_z is the phase constant in the direction of propagation. For a given f, the propagation constant is determined by finding k_z such that (25) is satisfied. There will be several values of k_z for each f corresponding to different order modes. The cutoff frequencies for the different modes may be obtained by searching for f such that $\det |H| = 0$ when $k_z = 0$. In general, $\det |H|$ is complex. So (25) implies that

$$\text{Re } [\det H] = 0 \tag{26}$$
$$\text{Im } [\det H] = 0. \tag{27}$$

The expansion set used to obtain (23) is only an approximation to the exact current sources. Due to this approximation, the values of k_z needed to satisfy (26) and (27) are, in general, slightly different. Therefore, an adequate approximate solution is obtained by requiring that

$$|\det (H(f,k_z))| = \text{minimum}. \tag{28}$$

In actual numerical calculation, a few spurious roots occur in the solution of (25). The actual roots are identified by the following three criteria: 1) k_z^0 that gives the deepest local minimum in $|\det H|$, 2) real and imaginary parts of $\det H$ should change sign near k_z^0, and 3) the difference in the values of k_z satisfying (26) and

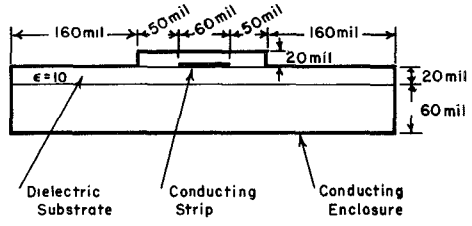

Fig. 5. Cross section for channelized suspended microstrip

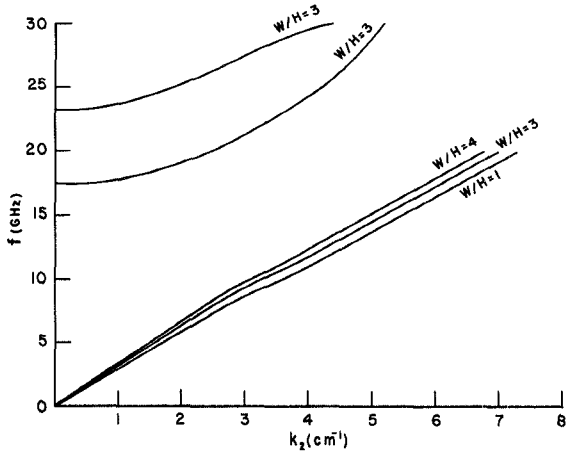

Fig. 6. Dispersion characteristics for channelized suspended microstrip. W—width of the conducting strip and H—height of the channel above it.

(27) is smallest. Also, the spurious roots shift appreciably when the number of segments in a contour is changed [1].

To illustrate the accuracy of the present method, results computed for a shielded-microstrip cross section shown in Fig. 3 are plotted in Fig. 4. The calculated dispersion characteristics of the fundamental and higher order even-symmetry modes agree reasonably well with the theoretical results in [2] and [4]. Although only even-symmetry modes are shown in Fig. 4, the method is applicable to all types of modes, symmetric or otherwise.

We next show the dispersion characteristics of a channelized suspended microstrip [7]. The cross section of the structure is shown in Fig. 5. The channel located above the conducting strip helps suppress higher order mode propagation. The structure has two additional useful features: 1) reduced dissipation loss [8], and 2) easier fabrication due to wider strip widths for 50-Ω impedance level. The calculated dispersion curves are shown in Fig. 6. The lower three curves represent the fundamental mode for three different values of W/H (= 1, 3, 4), the ratio of the width of the conducting strip, and the height of the channel above it. The upper two curves are two higher order (even symmetry) modes for $W/H = 3$. The associated TEM phase constants in air and dielectric material ($\varepsilon_r = 10.0$) are shown in the figure for reference. As can be seen in Fig. 6, the phase constants for the fundamental mode at lower frequencies are nearer to that in air and at high frequencies go towards the values for the dielectric medium. The cutoff frequencies for the next two even-symmetry higher order modes are 17.2 GHz and 27.4 GHz, respectively.

V. Discussion

The computer-aided analyses described in this short paper can determine the dispersion and higher order mode characteristics for a wide variety of transmission structures having different geometries and material parameters. The analysis includes the effects on propagation due to an arbitrarily shaped conducting enclosure. The analysis presented here can provide design information for planar transmission media which employ composite conductor and/or dielectric materials. The analysis can be readily extended to determine other propagation characteristics such as electric and magnetic field distributions, modal currents, impedance parameters, and dissipation losses.

References

[1] A. Farrar and A. T. Adams, "Computation of propagation constants for the fundamental and higher order modes in microstrip," *IEEE Trans. Microwave Theory Tech.*, vol. MTT-24, pp. 456–460, July 1976.

[2] E. Yamashita and K. Atsuki, "Analysis of microstrip-like transmission-like transmission lines by nonuniform discretization of the integral equations," *IEEE Trans. Microwave Theory Tech.*, vol MTT-24, pp. 195–200, Apr. 1976.

[3] G. Essayag and B. Sauve, "Study of higher order modes in a microstrip structure," *Electron. Lett.*, vol. 8, no. 23, pp. 564–566, Oct. 1972.

[4] R. Mittra and T. Itoh, "A new technique for the analysis of the dispersion characteristics of microstrip lines," *IEEE Trans. Microwave Theory Tech.*, vol. MTT-19, pp. 47–55, Jan. 1971.

[5] R. F. Harrington, *Time Harmonic Electromagnetic Fields*. New York: McGraw-Hill, 1961, pp. 106–110.

[6] ——, *Field Computation by Moment Methods*. London, England: Macmillan, 1968.

[7] A. K. Ganguly and B. E. Spielman, "Dispersion in arbitrarily-configured dielectric loaded transmission structures," in *1977 IEEE/MTT-S Int. Microwave Symp. Dig* (San Diego, CA), to be published in 1977.

[8] B. E. Spielman, "Computer-aided analysis of dissipation losses in isolated and coupled transmission lines for microwave and millimeter wave integrated-circuit applications," Naval Research Laboratory, Washington, DC, NRL Rep. 8009, p. 28, July 1976.